

Spectral Analysis of Growth in Spatial Lotka-Volterra Models

K.A. Hawick

Computer Science, Institute for Information and Mathematical Sciences,
Massey University, North Shore 102-904, Auckland, New Zealand

email: k.a.hawick@massey.ac.nz

Tel: +64 9 414 0800 Fax: +64 9 441 8181

March 2010

ABSTRACT

The Lotka-Volterra coupled system of equations describing relationships between predators and prey has been applied to a number of spatial biological and ecological models by several authors. The equations need to be time-integrated for long times on a large system to fully appreciate the complex bulk behaviour that ensues spatially. This paper applies some spectral analysis methods to spatial Lotka-Volterra models to study length scales and phased-locked spatial wave patterns at early and long time scales. We employ a custom simulation code that supports near-interactive time study of model systems of around 100,000 spatial cells, and that are time-integrated stably for up to 10,000 iterations. We report on spectral image analysis and numerical scattering experimental techniques. These suggest emergent and phase transitional behaviour in the parameters of the spatial Lotka-Volterra model

KEY WORDS

Lotka-Volterra; partial differential equations; spectral analysis; phase transitions; ecological model.

1 Introduction

Predator-prey relationships form the basis for modelling complex systems in environmental and ecological applications [1]. The Lotka-Volterra system of coupled differential equations [2, 3] can be solved numerically to demonstrate the boom-bust periodic oscillatory behaviour of the relative populations. The model has also

been successfully applied in other applications areas - such as blood vessel formation [4] - where two coupled competing agencies are involved.

There are a number of ways to incorporate spatial effects into the Lotka-Volterra equations. One suggestion due to Sprott is to form a simple spatial average of the cross coupling term [5] that feeds into each equation. The average could be over the nearest neighbours inclusive of the central site or exclusive of it. Another approach is to incorporate a properly normalised diffusive term [6–9] using the Laplacian ∇^2 operator. This can be implemented on a spatial mesh as a five-star stencil operation. We investigate both these variants in Sections 4 and 5. The diffusive approach gives rise to a set of coupled partial-differential equations (PDEs).

A number of authors have investigated spatial effects in the Lotka-Volterra system based on these diffusion ideas [10–13] and there has been considerable recent interest in variations of the model using discrete and Monte-Carlo techniques [14–17] in addition to use of PDE approaches. Generally it is necessary to consider quite large spatial systems - PDEs on a quite large grids and time-integration of the equations for several thousand time steps. To this end we have developed a custom simulation code (in C++) that supports large mesh sizes and which employs a fourth-order time-integration method allowing stable integration over relatively long simulation times. In addition to a framework that supports averaging results over many independently randomly seeded runs of the model we include spectral analysis techniques that allow construc-

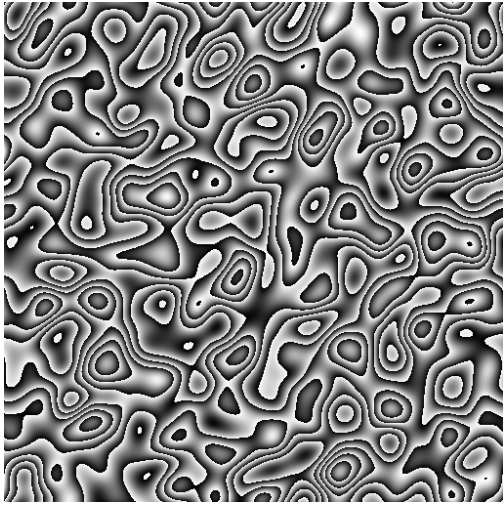


Figure 1: Spatial Lotka-Volterra system at time 2048×0.05 after random start on 512×512 square periodic grid.

tion of the Fourier images of the equation variables and their combination to construct numerical scattering experiments. Small-angle scattering [18] is a technique used in materials science [19], and it allows study of effects in a bulk field that would otherwise be difficult to spot or measure.

The Lotka-Volterra system [20] has also attracted interest [21, 22] as a framework for studying non-linear effects [23], noise [24], and relationships between microscopic behaviour and microscopic properties [25] in complex systems. Our interest in the Lotka-Volterra system stems from its use as a framework for studying growth and fluctuations [26] in complex systems. Other authors have observed that the spatial system is a rich source of spatio-temporal fluctuations [27] and spatial variability [28]. Discrete models of predator-prey systems [29] also produce complex spatial emergent patterns such as spirals [30] and wavefronts.

We show an example of the spatial wave fronts that oscillate between boom and bust in our simulated spatial Lotka-Volterra system in Figure 1. The spatial structures are readily measured at medium to long times, such as in the example shown for time $t = 2048 \times 0.05 \approx 100$. However, in this present paper we employ spectral methods to investigate the quantitative properties of wavefront length scales at the very **early stages** of the Lotka-Volterra spatial system when direct mea-

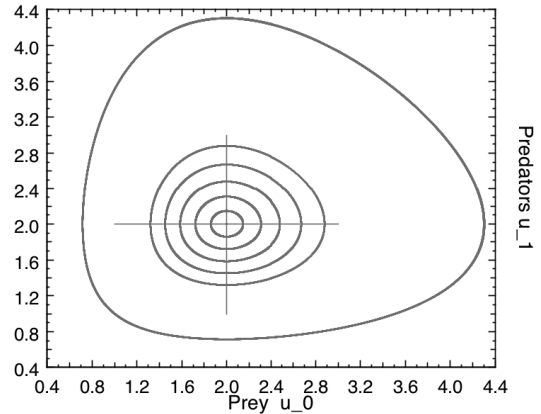


Figure 2: A typical set of Lotka-Volterra orbits in 2-species phase space, where the predator population phase-lags the prey by 90 degrees, manifested in boom-bust cycles.

surements on the field model are more difficult.

In Section 2 we describe the Lotka-Volterra system of coupled ordinary equations and how a spatial model can be established using coupled partial differential equations. We discuss algorithms and techniques for calculating numerical scattering intensities of the model configuration in Section 3. Some selected results are presented alongside a discussion of the length scales present in the spatial model in Sections 4 for the spatial averaging model and in Section 5 for the reaction-diffusion formulated model. Finally a summary, some tentative conclusions and some areas for further work are presented in Section 6.

2 Lotka-Volterra Equations

The Lotka-Volterra system of equations is usually written in terms of a n -vector \mathbf{u} of relative populations of the n species in the system as:

$$\frac{d\mathbf{u}}{dt} = \mathcal{F}(\mathbf{u}) \quad (1)$$

Which is often written in expanded form for a two-species system as:

$$\begin{aligned} \frac{du_0}{dt} &= Au_0 - Bu_0u_1 \\ \frac{du_1}{dt} &= Du_0u_1 - Cu_1 \end{aligned} \quad (2)$$

where the generalised interaction operator \mathcal{F} is limited to the four terms shown with simple positive coefficients A, B, C, D . It is useful to fix ideas and think of a simple predator prey system such as “rabbits and foxes” where u_0 is the population of prey or “rabbits” and u_1 is the population fraction of predators or “foxes.” This system has been well studied and is known to have a fixed point at $(x, y) = (\frac{D/C}{A/B})$. The implications of this are that a model system, initialised at some arbitrary point (x_0, y_0) will orbit around the fixed point for suitable non-zero values of A, B, C, D .

These four parameters can be interpreted in terms of the rabbit-fox predator-prey model as follows:

A is the (exponential) prey growth rate

B is the rate predators kill prey

C is the growth rate of predators from killing prey

D is the (exponential) death rate of predators

and are expressed this way as positive values. We adopt the convention most reported in the literature and set any self-interaction terms - squared terms including u_0u_0 or u_1u_1 - in the equations to have zero coefficients.

Figure 2 shows the typical fixed point attractor for the Lotka Volterra equations for the values: $\{A = 1, B = 0.5, C = 0.5, D = 1\}$. Any spatially isolated Lotka-Volterra cell with two species prey and predators shown on the x- and y-axes respectively, will orbit the fixed point anti-clockwise if initialised in the region of the fixed point. The figure shows points that have been initialised at $(1, 1), (1.5, 1.5), (1.6, 1.6), \dots, (2.0, 2.0)$ which give rise to equation trajectories that are seen to orbit the fixed point at $(2.0, 2.0)$, or stay at it.

We are interested in formulations of this coupled (pair) or equations that extend to a spatial field - such as a two-dimensional square grid, so that each cell has population variable for the fraction of predators and prey on it. We further want to find a realistic way to couple the cells spatially so that the predators and prey are effectively moving around the system but that the number of a particular species is conserved by the spatial operation, even although it will oscillate and change in time.

One form is:

$$\begin{aligned} \frac{du_0(\mathbf{r})}{dt} &= Au_0(\mathbf{r}) - B \langle u_0(\mathbf{r}) \rangle_{\mathbf{r}} u_1(\mathbf{r}) \\ \frac{du_1(\mathbf{r})}{dt} &= Du_0(\mathbf{r}) \langle u_1(\mathbf{r}) \rangle_{\mathbf{r}} - Cu_0(\mathbf{r}) \end{aligned} \quad (3)$$

where the spatial average $\langle \dots \rangle_{\mathbf{r}}$ is over the local region of physical space $\mathbf{r} = (x, y)$ in two dimensions and could be taken as the nearest neighbour average on a two-dimensional grid-based space for example. The average could be weighted by distance to include next-nearest neighbours using a weight stencil to control the diffusive influence or a reaction-diffusion process could be incorporated to make species attract or repel. We experimented with this form of spatial averaging as discussed below in Section 4.

A more useful form is:

$$\begin{aligned} \frac{du_0(\mathbf{r})}{dt} &= \mathcal{O}(u_0(\mathbf{r})) + Au_0(\mathbf{r}) - Bu_0(\mathbf{r})u_1(\mathbf{r}) \\ \frac{du_1(\mathbf{r})}{dt} &= \mathcal{O}(u_1(\mathbf{r})) + Du_0(\mathbf{r})u_1(\mathbf{r}) - Cu_0(\mathbf{r}) \end{aligned} \quad (4)$$

where a spatial operator \mathcal{O} can either be formulated as a spatial average as above, or can simply be taken as the Laplacian operator ∇^2 which then turns equation 5 into a reaction-diffusion equation system, based still upon the Lotka Volterra interactions. This approach is the most interesting as it gives rise to the spatial wave structures discussed in Section 5.

The work reported here makes use of periodic boundary conditions and the fourth-order Runge-Kutta time integration method for each spatial cell of variables.

3 Spectral Analysis & Numerical Scattering

Scattering experiments in materials science can use neutrons or x-rays or other particles. The essential physics is much the same and the end result is that a scattering experiment using an incident beam of particles can be used to probe the bulk average properties of a real sample. The scattering pattern formed by collecting the scattered particles in suitable detectors can give quantitative indications of the size and sometimes shape of spatial fluctuations and structures that are forming in the material. In the numerical simulation, a computation of the scattering pattern is possible and this can reveal properties of the simulated data field that would otherwise be hard to extract and observe. We give a brief derivation of the scattering formula.

A neutron scattering experiment conducted on a sample with volume V with scattering angle Ω and scattering cross-section (probability) of σ is given by:

$$\frac{d\sigma}{d\Omega} \approx (\rho_p - \rho_m)^2 \frac{1}{V} \left| \int_V e^{i\mathbf{Q}\cdot\mathbf{r}} d\mathbf{r} \right|^2 \quad (5)$$

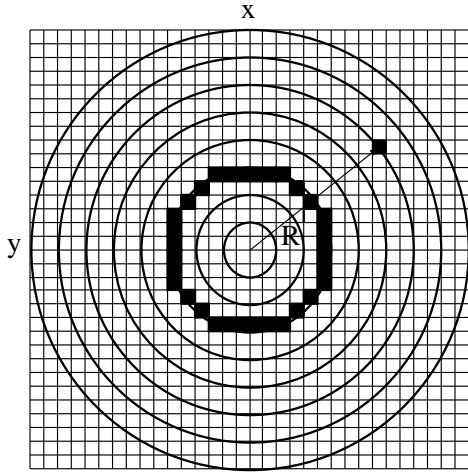


Figure 3: The circular binning scheme for the two dimensional scattering pattern. Values in Q-space are converted to radial average values, by binning around circles of constant $q = |Q|$. Resolution is limited at lower $|Q|$ values by the Cartesian approximation to a circle.

The term $(\rho_p - \rho_m)^2$ is the difference between the densities of the phase of interest and the background density and is known as the small angle scattering contrast, denoted as $\Delta\rho^2$. A large value of $\Delta\rho^2$ gives higher *relative* scattering intensity from the precipitate phase. Equation 5 can then be rewritten as:

$$\frac{d\sigma}{d\Omega} \approx (\rho_p - \rho_m)^2 \frac{1}{V} S(\mathbf{Q}) \quad (6)$$

which defines the structure function as:

$$S(\mathbf{Q}) = \left| \int_V e^{i\mathbf{Q}\cdot\mathbf{r}} d\mathbf{r} \right|^2 \quad (7)$$

which is strictly a dimensionless quantity.

For the purposes of this paper, we can treat the $S(\mathbf{Q})$ as a scattering intensity and which corresponds to the Fourier transform of the “contrast” or the physical configuration in the model system. We can take the contrast as simply the value of the field. So $S(Q)$ or $I(q_x, q_y)$ can be computed by a two-dimensional Fast Fourier Transform (FFT) of the data field u_0 or u_1 . In practice since the two variables are related though the phase coupling for the Lotka Volterra system, we find little difference in whether the FFT is computed by u_0 , or u_1 for the work reported here.

Some typical results of these numerical scattering images are presented and discussed below in Section 5. However, it is useful to consider the circular average - replacing the wave-vector $Q = (q_x, q_y)$ with a single wave number q which is inversely related to a spatial length l scale by $q \approx 2\pi/l$.

Figure 3 shows how a circular binning scheme can be used to obtain the numerical scattering as a function of the one-dimensional wave number q . This analysis is discussed in greater detail in [31]. We use this technique to obtain data shown below in figure 10 and 6.

4 Spatial Averaged Results

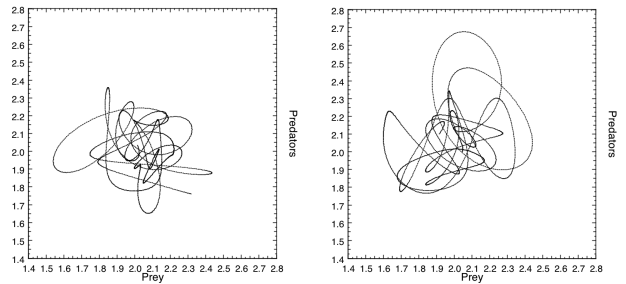


Figure 4: Random walks traced out by Spatial Lotka Volterra system using exclusive average with 2 species system, 2048 steps, $h = 0.1$, $a = d = 1$, $c = b = 0.5$, fixed point at 2,2, at cell 0 left, at cell 1, right.

A number of experiments were carried out on systems of size 128×128 spatial cells arranged on a square mesh with periodic boundary conditions. The systems were initialised randomly and time integrated for up to 10,000 time-steps using various step sizes. Most of the work used a step size of $h = 0.01$ and parameters for equation 3 of $A = D = 1$; $B = C = 0.5$ (and this with a fixed point at $(2, 2)$), unless stated otherwise.

There are a number of ways of applying spatial coupling as discussed in Section 1. Spatial coupling will force the individual cells to behave differently to the regular oscillatory behaviour they would exhibit if spatially isolated. Figure 4 shows some typical tracks in phase space arising from using a different spatial operator - the exclusive average over the four neighbouring cells. Although over-all the model is stable and individual cells remain in (complex) orbits around the fixed point, the resulting spatial patterns are not interesting and remain random.

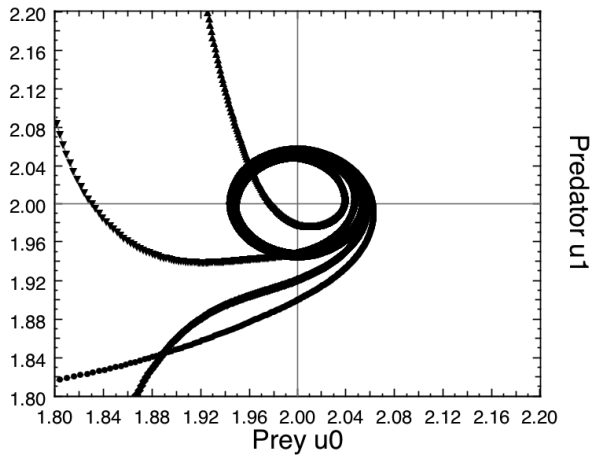


Figure 5: Four of the spatial cells converging to a stable orbit around the fixed point. Since they are nearby they have locked to similar orbits.

The data presented in Figure 5 shows four typical tracked cells in a 128×128 model system. The initial values are chosen randomly on a uniform interval around the fixed point, and the spatial diffusion coupling of the model drives individual cells towards the stable orbit of the attractor.

5 Spatial Diffusion Results and Discussion

Figure 10 shows screen-dump image representations of the prey (u_0) and predator (u_1) spatial variables, shaded according to their values on an intensity gray-scale of $[1.5, 2.5]$. In between the scattering intensity $S(q_x, q_y)$ is shown also displayed on an intensity-based gray-scale. Initially the system is random with no discernible spatial features and gradually as the spatial coupling exerts it influence the oscillating cells phase lock together and the waves of boom-bust Lotka-Volterra behaviour appear. The spatial period of these waves grows across the system with time. The length-scales will continue monotonically - **on average** although spatial fluctuations are present and allow regions to join up or to disperse. Generally the time behaviour is over logarithmic time scales and is not linear. Over medium to long times the effect can be seen directly in the configurations but it is not easy to observe directly at early-to-medium time-scales ($t \approx 1 = 1000 \times 0.001$).

The scattering image however shows that considerable changes **are** occurring at early to medium times in the system. The 2-d scattering image starts random, then forms a slowly collapsing circular pattern that gradually shifts the power to lower wave vector values, indicating rising spatial structure in the system. The spatial Lotka-Volterra scattering pattern are not collapsing rings or halos as is seen in spinodal decomposition systems such as the Cahn-Hilliard model [31]. Instead the Lotka-Volterra spatial model appears to have a spread of spatial sizes present. The connected waves oscillate and represent the long-range spatial structure and a slow shift to dominance at lower q . The small-scaled features are hard to see in either the direct configurations or the spectral images, but can be discerned from a plot on log-log scales of the circularly averaged spectral image.

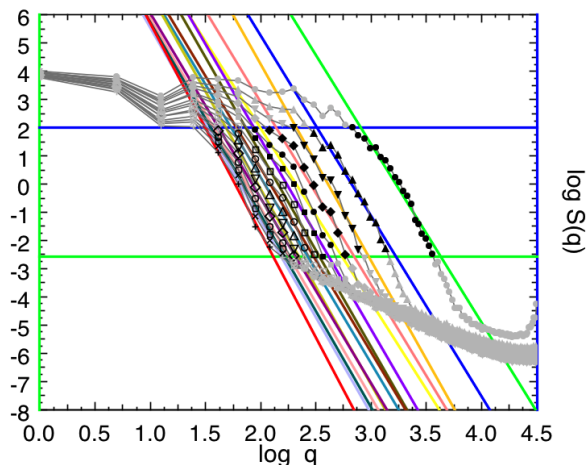


Figure 6: Circular Averaged Scattering Patterns (for the model with $A = 1.0$) with straight lines showing the fitted slopes, which have mean -6.7 ± 0.3 over region shown.

Figure 6 shows the circular-averaged Scattering intensity $I(q) = \langle I(\mathbf{q}) \rangle_\theta$ computed using the 2-dimensional Fast Fourier Transform. The shoulder of the scattering intensity plots has a mean slope of -6.7 ± 0.3 independent of time t , but the lines shift to lower y-intercepts with time. We can infer an approximate relationship $l = 2\pi/q_0$ where $\log q_0(t)$ are the intercepts with the x-axis at a convenient horizontal line such as at $\log S(q) \equiv 0$. This data set is too noisy to infer a definite relationship, but it does suggest monotonically increasing spatial relationship between

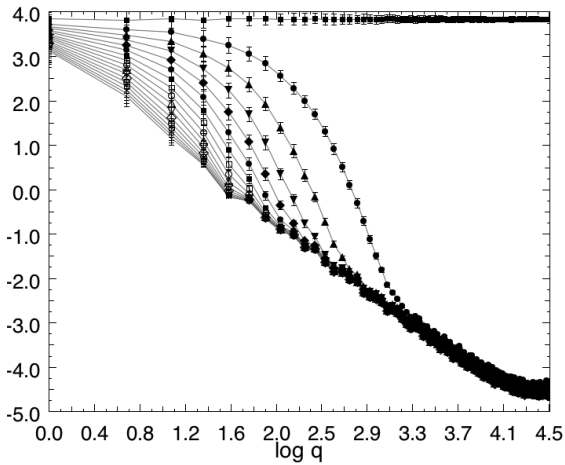


Figure 7: Similar experiment and data as in Figure 6 except here, the data are averaged over 100 independent runs.

the characteristic length scale and time. Combining results from more runs of larger systems might yield sufficient statistical information to determine whether this is a power law or a logarithmic relationship.

Figure 8 shows the characteristic length computed using the approach above where we have scaled the l values by the lattice length 128. The relationship appears to be approximately logarithmic in time.

The long tail at extreme right of the plot of $S(q)$ has a well-defined slope that gives information on the high- q or small-sized features of the system. A least-squares fit for the base parameter model of $A = D = 1; B = C = 0.5$ indicates a slope of -1.8 ± 0.01 . Porod's law [32] suggests the negative of this slope indicates an approximate effective dimensionality of the small features in the system. In this case it is a fractional dimension smaller than 2, but which is a feasible indicator of the small local patches of predator or prey.

Figure 7 shows the result of performing the same experiment as above but averaging the scattering data over 100 separate and independently random seeded runs. Statistically the same spatial patterns occur but it is meaningful to average the scattering pattern as the smooth data in Figure 7 indicates.

Varying the prey growth parameter A to higher values such as 1.5 makes the fitted exponent change to -1.9 ± 0.01 and decreasing the prey growth parameter changes the fitted slope to -1.7 ± 0.02 . This is consistent with a higher growth rate causing more dense

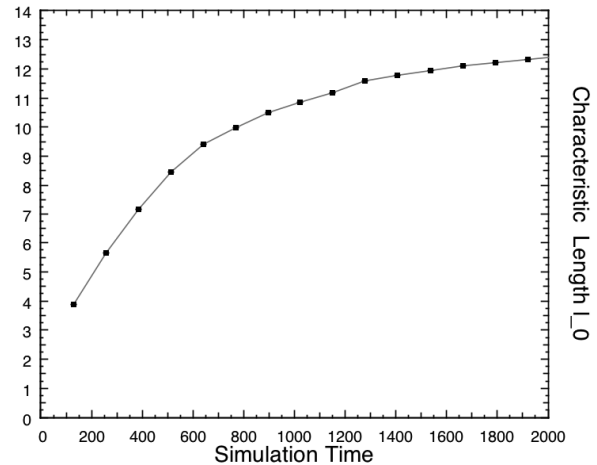


Figure 8: Characteristic length scale as it varies with time, computed for the system with $A = 1.0$.

populations locally and leading to denser local regions in the model with an effective fractional dimension of $d_f \approx 1.9$, or lowering it to $d_f \approx 1.7$ when growth of prey is less pronounced. A more systematic exploration of the parameter with large model systems and greater number of runs might lead to a more systematic relationship between the rate equation parameters A, B, C, D and the bulk length scales and their effective dimensionalities.

It would also be interesting to verify this relationship carries over to a three-dimensional system where effective local dimensionalities in the region $d_f \approx 2.5$ might be expected.

Figure 9 shows configuration snapshots of the predator population (u_1) system with different values of the prey growth rate $A = 1.0, 0.5, 0.25, 1.25$. Generally it is seen that the spatial features are smaller and the oscillations more rapid if the prey population growth is reduced. Lowering A shifts the fixed point to the left on the phase plots and raising it shifts it to the right. Physically one might intuit that lower growth rates of prey makes the system more vulnerable to spatial fluctuations such as food shortages and local extinctions. Higher prey growth might be expected to dampen the effect of local populations and support growth of larger spatial regions. However as the lower right image in Figure 9 indicates that raising A also leads to more rapidly changing spatial waves in the system. It appears that too much prey will also drive the system to frantic oscillation spatially. We might anticipate that a detailed

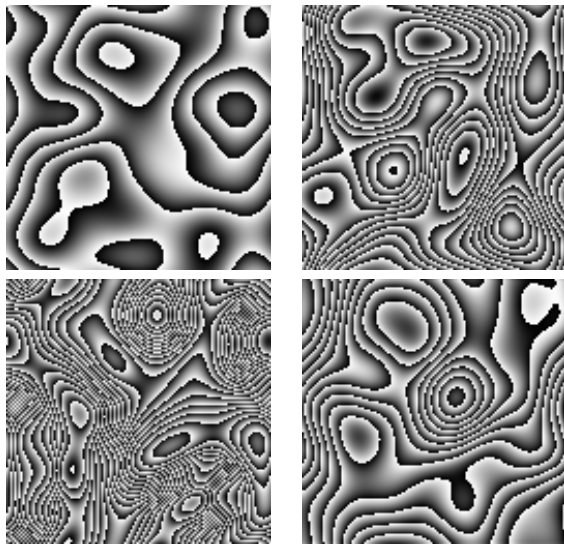


Figure 9: Predator configurations at different Prey growth rates: $A = 1.0, 0.5, 0.25, 1.25$ for top left, top-right, etc respectively. All were run for 2048 time steps, with $h = 0.05$, with parameters $B = C = 0.5$; $D = 1$, on a periodic 128×128 Lattice, after initialisation around $(u_0 \in [1.5, 2.5], u_1 \in [1.5, 2.5])$ around the fixed point.

parameter investigation with larger systems and more runs might indicate a phase transition in the growth parameter.

6 Summary and Conclusions

We have described how the spatial Lotka-Volterra equations can be studied on a relatively large period mesh for long integration times using custom simulation codes. We have explored coupling mechanisms such as simple inclusive and exclusive neighbour averaging and found they give rise to individually stable behaviour but do not lead to phase-locking that can support large spatial structures such as waves. Using a proper Laplacian in the spatial equations couples cells together so that long-range spatial structures can develop, propagate and oscillate. The oscillations lead to the merging and dissipation of spatial waved structures which continue to oscillate together, phase-locked by the diffusive coupling between spatial cells.

We have used spectral methods from material science

that are based on small-angle scattering and have presented calculated scattering images of the evolving spatial model. The scattering patterns illustrate effects that are not discernible in the early to medium time-scales of the model and also gives a quantitative estimate of the fractal or effective dimension of small scale phenomena and features at all time scales.

It seems likely that we can extend our simulation codes to enable study Lotka-Volterra systems in three (Euclidean) dimensions and also to consider systems with more than two species present [33]. The spatial Lotka-Volterra system is finding uses in many studies of population an ecological systems. We believe these spectral methods may give fresh insights into other models.

References

- [1] Standish, R.K.: Cellular ecolab. *Complexity International* **6** (1998) 1–12
- [2] Lotka, A.J.: *Elements of Physical Biology*. Williams & Williams, Baltimore (1925)
- [3] Volterra, V.: *Variazioni e fluttuazioni del numero d'individui in specie animali conviventi*. *Mem. R. Accad. Naz. dei Lincei, Ser VI* **2** (1926)
- [4] Petitet, G., McElwain, D., Norbury, J.: Lotka-volterra equations with chemotaxis: walls, barriers and traveling waves. *IMA J. of Maths. Applied in Medecine and Biology* **17** (2000) 395–413
- [5] Sprott, J., Wildenberg, J., Azizi, Y.: A simple spatiotemporal chaotic lotka volterramodel. *Chaos, Solitons and Fractals* **26** (2005) 1035–1043
- [6] Lou, Y., Martinex, S., Nicholas, W.M.: On 3 x 3 lotka volterra competition systems with cross diffusion. *Discrete and Continuous Dynamical Systems* **6** (2000) 175–190
- [7] Le, D.: Cross diffusion systems on n spatial dimensional domains. *Electronic Journal of Differential Equations* **10** (2003) 193–210 *Proc. Fifth Mississippi State Conference on Differential Equations and Computational Simulations*.
- [8] Martinez, S., Nicholas, W.M.: Periodic Solutions for a 3 x 3 Competitive System with Cross-Diffusion. *Discrete and Continuous Dynamical Systems* **15** (2006) 725–746
- [9] Gambino, G., Lombardo, M., Sammartino, M.: A velocity diffusion method for a Lotka-Volterra System with nonlinear cross and self-diffusion. *Applied Numerical Mathematics* **59** (2009) 1059–1074
- [10] Satulovsky, J.E.: Lattice lotkavolterra models and negative cross-diffusion. *J. Theor. Biol.* **183** (1996) 381–389

- [11] Neuhauser, C., Pacala, S.: An explicitly spatial version of the lotka-volterra model with interspecific competition. *The Annals of Applied Probability* **9** (1999) 1226–1259
- [12] Satulovsky, J.E., Tome, T.: Spatial instabilities and local oscillations in a lattice gas lotka-volterra model. *J. Math. Biol.* **35** (1997) 344–358
- [13] Caristi, G., Rybakowski, K.P., Wessoler, T.: Persistence and spatial patterns in a one-predator-two-prey lotka-volterra model with diffusion. *Annali di Matematica pura ed applicata* **CLXI** (1992) 345–377
- [14] Szabo, G., Czarán, T.: Phase transition in a spatial Lotka-Volterra model. *Phys. Rev. E* **63** (2001) 061904–1–4
- [15] Malcai, O., Biham, O., Richmond, P., Solomon, S.: Theoretical analysis and simulations of the generalized lotka-volterra model. *Phys. Rev. E* **66** (2002) 031102
- [16] Spagnolo, B., Fiasconaro, A., Valenti, D.: Noise induced phenomena in lotka-volterra systems. *Fluctuation and Noise Letters* **3** (2003) L177–L185
- [17] Fiasconaro, A., Valenti, D., Spagnolo, B.: Nonmonotonic behavior of spatiotemporal pattern formation in a noisy lotka-volterra system. *Acta Physica Polonica B* **35** (2004) 1491
- [18] Windsor, C.G.: An Introduction to Small Angle Neutron Scattering. *J. Appl. Cryst.* **21** (1988) 582–588
- [19] Kosterz, G.: Small angle neutron scattering - Metallurgical applications. *Mat. Sci. Forum* **27** (1988) 325–344
- [20] Cushing, J.: Periodic Lotka-Volterra Competition Equations. *J. Math. Biol.* **24** (1986) 381–403
- [21] Ackland, G., Gallagher, I.: Stabilization of large generalized lotka-volterra foodwebs by evolutionary feedback. *Phys. Rev. Lett.* **93** (2004) 158701–1–4
- [22] Swart, J.: Behavioural Sensitivity of the Lotka-Volterra Model. In: *Mathematical Ecology*. Wiley (1977) 379–390
- [23] Yang, M., Lee, S., Kim, S.K., Shin, K.J., Ryu, M.H., Lee, S.H., Lee, D.J.: A Nonlinear theory for the Lotka-Volterra Model with an External Input. *Bull. Korean Chem. Soc.* **13** (1992) 560–565
- [24] Leung, H.: Stochastic transients of noisy lotka-volterra model. *Chinese Journal of Physics Letters A* **29** (1991) 637–652
- [25] Poggiale, J.: Lotka-Volterra’s Model and Migrations: Breaking of the Well-Known Center. *Mathl. Comput. Modelling* **27** (1998) 51–61
- [26] Shabunin, A., Efimov, A.: Lattice Lotka-Volterra Model with Long Range Mixing. *Eur. Phys. J. B* **65** (2008) 387–393
- [27] Mobilia, M., Georgiev, I.T., Tauber, U.C.: Phase transitions and spatio-temporal fluctuations in stochastic lattice lotka-volterra models. *J. Stat. Phys.* **128** (2007) 1572–9613
- [28] Dubravný, U., Tauber, U.C.: Spatial variability enhances species fitness in stochastic predator-prey interactions. *Phys. Rev. Lett.* **101** (2008) 258102–1–4
- [29] Hawick, K.A., Scogings, C.J.: A minimal spatial cellular automata for hierarchical predator-prey simulation of food chains. Technical Report CSTN-040, Computer Science, Massey University (2010)
- [30] Hawick, K.A., Scogings, C.J., James, H.A.: Defensive spiral emergence in a predator-prey model. *Complexity International* (2008) 1–10
- [31] Hawick, K.A.: Domain Growth in Alloys. PhD thesis, Edinburgh University (1991)
- [32] Martin, D.G.: Observed deviations from Porod’s Law that are due to the non-ideal geometry of a small angle scattering experiment. MPD/NBS/137 137, Harwell Laboratory, MPMD, Harwell Laboratory, Oxon. , UK. (1980)
- [33] Szabó, G., Ariel Sznajder, G.: Phase transition and selection in a four-species cyclic predator-prey model. *Phys. Rev. E* **69** (2004) 031911

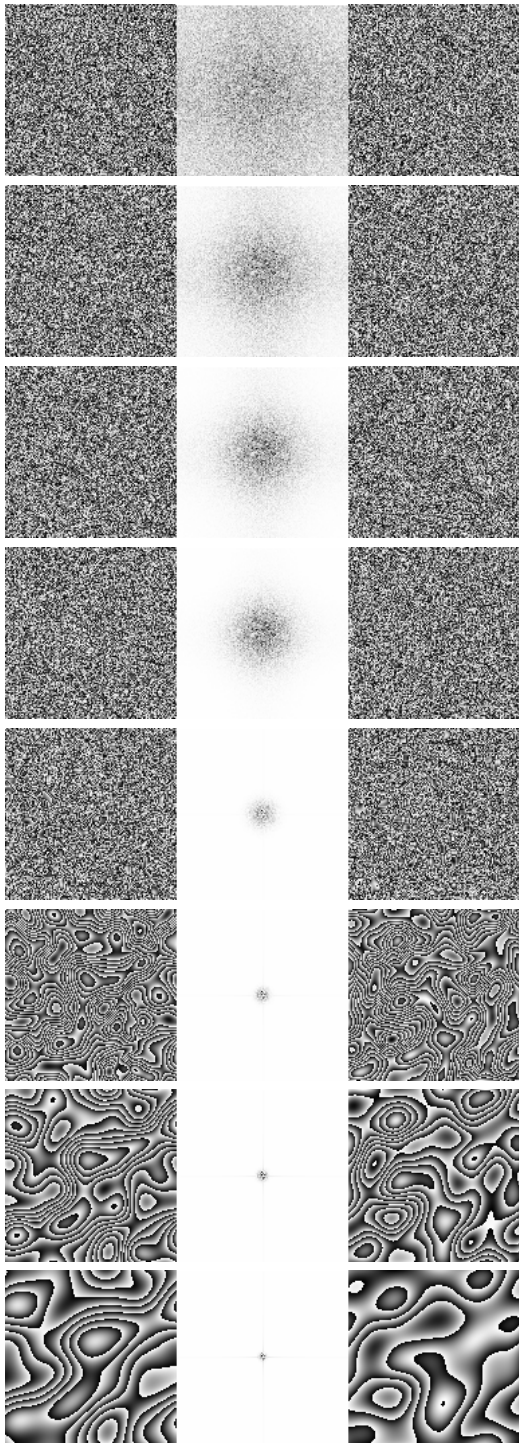


Figure 10: Spatial System configuration (u_0 on left, u_1 on right, with $I(q_x, q_y)$ in middle. Times shown top to bottom are: $t = 0.1, 0.2, 0.3, 1.0, 5.0, 25.0, 50.0, 100.0$ and were obtained with a time-step $h = 0.001$, for the first 3 and $h = 0.01$ for the remainder. The FFT reveals structure not directly visible in the early configurations. 9